THE ASTROPHYSICAL JOURNAL, 223:260–265, 1978 July 1

SPECTROSCOPY OF THE EXTREME-ULTRAVIOLET SOURCE FEIGE 24: THE BINARY ORBIT AND THE MASS OF THE WHITE DWARF

JOHN R. THORSTENSEN,*† PHILIP A. CHARLES,† BRUCE MARGON,‡ AND STUART BOWYER*†

Received 1977 August 22; accepted 1978 January 16

ABSTRACT

We report results of coudé spectroscopy of the extreme-ultraviolet white dwarf Feige 24. Radial velocities of the Hα, He I λ5876, and He I λ6678 emission lines, and the underlying M dwarf absorption features, were determined from spectrograms obtained with the Lick 3 m telescope. The velocities show a binary period of $4^{d}.2319 \pm 0^{d}.0015$. The emission-line and absorption-line velocities agree in phase, which indicates that the emission lines originate in the atmosphere of the M dwarf secondary as a result of reprocessing of the EUV radiation. After modeling this effect, we used the observed amplitude of the emission-line variability to place a lower limit on the orbital inclination. From these and other data we show that the mass of the white dwarf lies between 0.46 and 1.24 $M_{\odot}$. We briefly discuss some possible implications for the evolution of binary stars.

Subject headings: stars: binaries — stars: individual — stars: white dwarfs — ultraviolet: general

I. INTRODUCTION

Feige 24 (Feige 1958) has been shown by Margon *et al.* (1976) to be one of the hottest known white dwarfs. These authors detected the object in the 170–620 Å band using the extreme-ultraviolet (100–1000 Å) detector flown on board the *Apollo-Soyuz* Test Project in 1975 July. Interpreting their measurement in terms of pure hydrogen model atmospheres, they derived a temperature of 6×10^4 K. Far-ultraviolet photometry by Holm (1976) also implies a very high temperature for this star.

Feige 24 exhibits some remarkable optical properties. In the blue region, its spectrum contains sharp hydrogen Balmer and Ca II emission lines superposed upon the broad Balmer absorption of a normal DA white dwarf (Eggen and Greenstein 1965). The presence of this emission led Eggen and Greenstein to propose that the system is similar to an old nova, a close binary with emission lines arising from an accretion disk about a (possibly degenerate) primary. Further evidence for the binary nature of the system was given by Oke (1974), whose spectrophotometric measurements indicated the presence of a red component. With high-resolution spectrophotometry, Liebert and Margon (1977, henceforth LM) were able to classify the red component as M1 to M2 V on the basis of the TiO band strengths. LM also found the emission lines to be highly variable on time scales of ~1 day but to be sensibly constant on shorter time scales.

* Astronomy Department, University of California, Berkeley.

† Space Sciences Laboratory, University of California, Berkeley.

‡ Astronomy Department, University of California, Los Angeles.

In reviewing the available data, LM concluded that Feige 24 is probably not similar to an old nova, since it is not observed to be variable. The cause of the emission-line variability remained unclear; they suggested two possibilities. First, the M star may be a flare star and exhibit intrinsic spectral variations. In this case, one might expect the spectrum to be variable on more rapid time scales than observed. Second, it seemed possible that the intense EUV flux of the white dwarf causes the emission lines to arise on the EUV heated side of the M star. To clarify this issue, we undertook the following investigation.

II. OBSERVATIONS

We obtained 31 spectrograms on 14 different nights at the coudé focus of the Lick Observatory 3 m telescope, using the Varo image tube. These spectrograms cover the wavelength range 5850–6900 Å, at a dispersion of 33 Å mm^{-1}, and are detailed in Table 1. Calibration strips were applied during the exposures, and comparison lines were added near the beginning and end of each exposure.

The most prominent features visible on our spectrograms are narrow, symmetric emission at Hα, and weaker emission at He I λ5876 and He I λ6678. The emission strength varies widely, with all three emission lines varying together; on many spectra, only Hα is visible. In accordance with the observations of LM, the emission strength is nearly constant on any one night but varies from night to night. On some of the spectrograms, very weak Fe I, Ca I, Na I, and TiO absorption features are visible. These evidently arise from the M dwarf secondary; their weakness is due to filling in by the strong white dwarf continuum, which in this spectral region contributes 70%–80% of the light.

TABLE 1

EMISSION-LINE VELOCITIES

JD 2,440,000+	Velocity (km s^{-1})	Estimated Uncertainty (km s^{-1})	Phase	Adopted Nightly Average (km s^{-1})
2767.673.....	−11	±13	0.851	
2767.724.....	−3	12	0.854	−4
2767.759.....	+12	20	0.862	
2796.605.....	−21	30	0.678	
2796.639.....	−6	30	0.687	−8
2797.602.....	...		0.914	
2797.635.....	+36*	25	0.922	+36*
2798.602.....	+106	19	0.150	
2798.783.....	+123	11	0.193	+119
3061.944.....	+115†	10	0.378	+115†
3062.779.....	+28†	9	0.576	
3062.838.....	+17	6	0.589	
3062.895.....	+14	8	0.603	+15
3062.944.....	+12	8	0.615	
3063.761.....	−12	15	0.808	
3063.841.....	−11	12	0.826	−5
3063.898.....	+7	13	0.840	
3064.726.....	+53*	30	0.036	
3064.776.....	+63*	30	0.047	
3064.819.....	+74*	30	0.058	
3064.863.....	+82*	30	0.068	+75*
3064.903.....	+75*	30	0.077	
3064.943.....	+78*	30	0.087	
3116.679.....	+119	7	0.312	
3116.743.....	+101	8	0.327	+112
3119.731.....	+71	15	0.033	+71
3121.714.....	+56	7	0.502	+56
3150.652.....	+112	12	0.340	+112
3151.668.....	+26	12	0.580	+26
3178.620.....	+13†	35	0.949	+13†

* Discarded from fit because of very large estimated uncertainty.

† Discarded from fit because of possible systematic errors.

III. RADIAL VELOCITIES

To obtain radial velocities, we scanned the spectrograms with the Berkeley Astronomy Department PDS microdensitometer and reduced these scans using an interactive computer program. The results for the emission lines are presented in Table 1. The uncertainties quoted in Table 1 were assigned subjectively by inspection of the line profiles. They represent extreme estimates of the possible effects of noise upon the placement of the line centers and do not refer to any systematic zero offset. Although care was taken to ensure the uniformity of these data, some of the velocities may suffer from identifiable systematic errors; these are indicated in Table 1. The range of quoted errors reflects primarily the greatly variable strength of the emission lines. The absorption-line profiles were in general far noisier than the emission-line profiles; their radial velocities are far less accurately determined. Within the large measurement uncertainties (typically ±40 km s^{-1}), the absorption and emission velocities always agree.

During any one night, the emission-line velocity remains nearly constant. When more than one line is present, the radial velocities of the different lines agree, although the He I λ5876 velocities are on average 11 km s^{-1} higher than the H velocities. This is probably a systematic error;[1] we assume so and adjust accordingly in the subsequent reduction. Because the radial velocity was essentially constant during any one night, we have averaged the velocities from each night in presenting our results.

Our 14 nights of data have allowed us to derive an ephemeris which is free of any ambiguities due to unknown numbers of cycles between the observations. We find that all of our radial velocities are well fitted by the function

$$v(t) = \gamma + K \sin [2\pi(t - t_0)/P] ,$$

with a weighted least-squares fit giving

$$P = 4^{d}.2319 \pm 0^{d}.0015 ,$$

$$K = 67.3 \pm 4.2 \text{ km s}^{-1} ,$$

$$\gamma = 55.2 \pm 3.9 \text{ km s}^{-1} ,$$

$$t_0 = 2443119^{d}.59 \pm 0^{d}.06 .$$

This fit did not include two points with possible systematic errors or data from the two nights with the largest estimated errors. The emission lines were quite weak during these nights, which made accurate measurements difficult. The nightly averages of radial velocity are shown together with the best-fit curve in Figure 1.

The errors quoted are 90% confidence intervals, derived using the procedure of Cash (1978) for error estimation of parameter subsets in the case of unknown variances. We take K and P to be dynamically interesting quantities, q in number, and γ and t_0 to be the $p - q$ uninteresting parameters. We then use the condition

$$\frac{(S_{\min})_{p-q}{}^{T}}{(S_{\min})_{p}} \leq 1 + \frac{q}{N - p} F(q, N - p, 0.9) ,$$

where the notation follows that of Cash, to construct 90% confidence intervals. The uncertainties quoted for γ and t_0 were derived by the standard method of solving for all the uncertainties simultaneously; a self-consistent set of error estimates for *all* the parameters results in estimated uncertainties for K and P slightly larger than those given above.

The elements above allow us to derive several interesting quantities with minimal assumptions. If we assume the velocity variations to be due to orbital motion, the random residuals to the best-fit sinusoid show the orbit to be circular. Although we have not derived formal upper limits, the small size of the residuals suggests that the eccentricity $e < 0.1$. The orbital radius of the emitting region must be at least $PK/2\pi = 3.9 \times 10^{12}$ cm $= 5.6\ R_{\odot}$. This is much larger than the M star, which should have a radius $\sim 0.6\ R_{\odot}$,

[1] The comparison lines near He I λ5876 are more widely spaced than in the region of the other lines. Consequently, tube distortions may easily explain such a systematic offset. The absolute values of the radial velocities should be accurate to ~15 km s^{-1} in well-defined spectral regions.

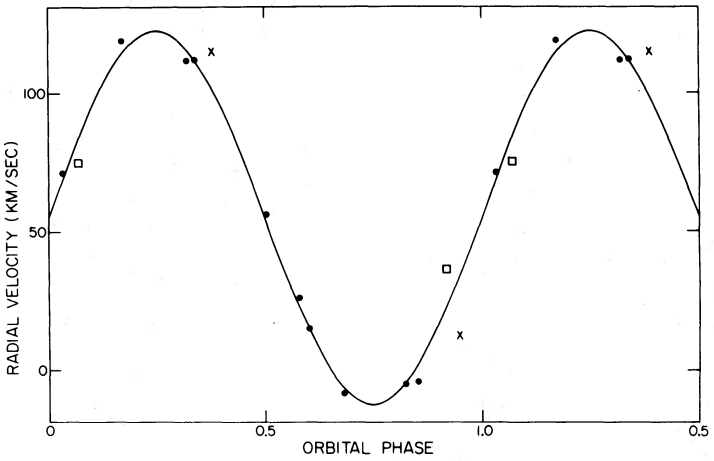

FIG. 1.—Nightly averages of the emission-line radial velocities (taken from Table 1) plotted against orbital phase. The points shown by crosses were discarded from the fit because of possible systematic errors; the squares indicate points that were not used because of their large estimated errors. The curve is the best-fit sinusoid to the remaining points.

assuming that it is on or near the main sequence. If the period of the emission-line velocity is the binary period, as we argue below, the stars themselves must be widely separated compared with their radii.

IV. EMISSION-LINE VARIATIONS

We find a strong correlation between the phase of the radial velocity variation and the strength of the emission lines. This correlation holds for all our coudé spectrograms, and also for all of the observations reported by LM. The sense of the correlation is as follows: While the radial velocity is decreasing, and the source of the emission is therefore on the more distant side of its orbit, the emission is strong. Conversely, as the radial velocity increases, the emission is weak.

To understand this more quantitatively, we measured equivalent widths of all emission lines visible on our calibrated spectrograms. We found the equivalent widths to repeat accurately from orbit to orbit, and to be symmetric about phases 0.0 and 0.5, within our margin of uncertainty. The equivalent widths of Hα are plotted against this orbital phase in Figure 2; the helium lines behave similarly when they are measurably strong.

All these observations strongly suggest that the emission lines arise from the reprocessing of EUV radiation. In this picture, as the M dwarf orbits the white dwarf, the EUV illuminated portion of the M dwarf that we see from Earth changes with orbital phase. This explains, qualitatively, both the sense of the effect and its demonstrated repeatability. The agreement of emission- and absorption-line velocities strongly supports this hypothesis.

V. SOME MODELS FOR INTERPRETING THE EMISSION-LINE VARIATIONS

In order to test the reprocessing hypothesis quantitatively and to show that further information can in principle be derived from our measurements, we consider here several models of the reprocessing geometry. We confine our attention to the Hα line, for which our measurements are most accurate. The assumptions common to all these models are as follows: (1) All of the emitting material is associated with the M star. (2) This material is confined to a layer in the star's atmosphere, with a thickness much less than R_M (the radius of the M star). (3) The emission spectrum of the M star is caused entirely by the reprocessing of EUV radiation; none of it is intrinsic.

Assumption 1 is equivalent to stating that there is no appreciable amount of gas between the two components of the binary system. Since in this model both stars lie deep within their tidal lobes, there can be no gravitationally driven mass flows. The stellar wind of the M star is unlikely to intercept an appreciable fraction of the EUV radation, even though the cross section for photoelectric absorption of EUV radiation by neutral hydrogen is large ($\sim 10^{-18}$ cm^2 [Cruddace *et al.* 1974]). If we demand that the wind intercept the same amount of EUV radiation as does the M star itself, we find that the wind must have a column density of *neutral* atoms near 10^{15} cm^{-2}, which in turn implies an implausibly large $n_{\rm H\,I} \approx 10^3$ cm^{-3} over the dimensions of the system.

We may justify assumption 2 by noting that ionized material cools efficiently at temperatures greater than $\sim 10^4$ K. Thus the material may not become hot enough to appreciably increase the scale height as compared with R_M. We adopt assumption 3 for simplicity: our data do not allow it to be verified directly.

We now consider the effects of making and varying several further assumptions which may not be justified as easily as assumptions 1 and 2.

Model A.—In this model, we assume that (A1) the emitting layer is optically thin to the emergent Hα radiation and (A2) each EUV photon gives rise to, on the average, f photons of Hα radiation. Assumption

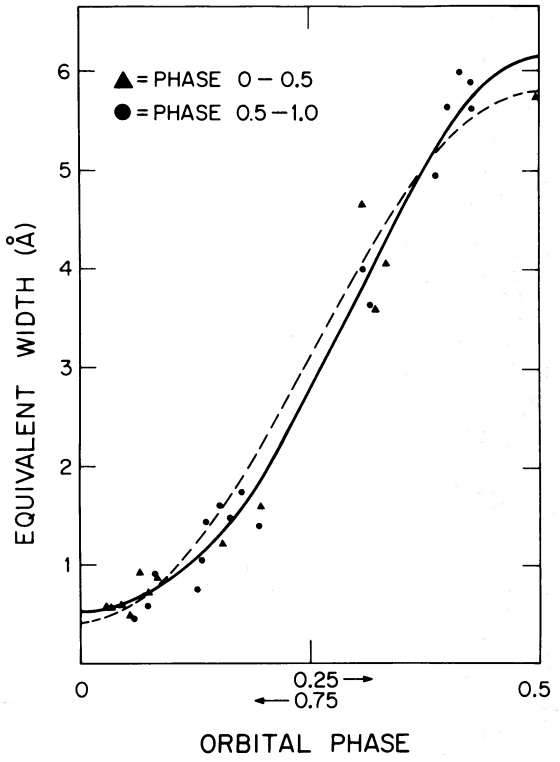

FIG. 2.—Equivalent widths of Hα emission as a function of orbital phase. The data have been folded around phase 0.5 to display their symmetry. Points from between phase 0 and 0.5 are plotted as dots, while points from between phase 0.5 and 1.0 are plotted as triangles. The dashed curve gives the prediction of models A and B, discussed in the text, for an orbital inclination of 60°. The solid curve gives the prediction of model C for an orbital inclination of 41°. Both curves have been scaled to fit the data.

A1 depends critically upon the extent to which trapped Lα photons populate the second level of hydrogen. Assumption A2, although certainly valid for radiative recombination at low density, might not be valid in this case, since the density at the base of the ionized layer is expected to be $\sim 10^{12}$ cm^{-3}. We arrive at this density by demanding that the number of recombinations of hydrogen to levels with $n \geq 2$ be equal in each column to the incoming EUV photon flux and by assuming that the ionized layer has the structure of an isothermal atmosphere at $T \approx 10^4$ K.

We may then calculate the strength of the Hα emission observable at Earth in the following manner: Consider a surface element ds on the EUV illuminated face of the M dwarf. It will absorb $N_{\rm EUV}(\hat{w}\cdot ds)/4\pi A^2$ photons of EUV radiation per unit time, where $N_{\rm EUV}$ is the number of EUV photons emitted per unit time by the white dwarf, $\hat{w}$ is a unit vector in the direction from the surface element to the white dwarf, and A is the distance between the surface element and the white dwarf. If this surface element is suitably oriented to be visible from Earth, it will produce a flux of Hα photons at Earth of $fN_{\rm EUV}(\hat{w}\cdot ds)/(4\pi AD)^2$, where D is the distance of the system. We have used assumption 3 in deriving this equation; we need not consider the radiative transfer of the outgoing Hα radiation. Finally we integrate to find

$$S_{\rm H\alpha} = \int_\Omega \frac{fN_{\rm EUV}(\hat{w}\cdot ds)}{(4\pi AD)^2} ,$$

where $S_{\rm H\alpha}$ is the photon flux of Hα radiation at Earth and Ω is the suitably oriented portion of the surface of the M dwarf. If we define $S_{\rm EUV}$ as $N_{\rm EUV}/4\pi D^2$, we may rewrite this expression in a distance-independent form as

$$\frac{S_{\rm H\alpha}}{S_{\rm EUV}} = \frac{f}{4\pi A^2}\int_\Omega \hat{w}\cdot ds .$$

Assuming that $R_M \ll A$, we may rewrite the above expression in terms of a geometrical factor $\Phi(\theta)$ as

$$\frac{S_{\rm H\alpha}}{S_{\rm EUV}} = f\left(\frac{R_M}{A}\right)^2 \Phi(\theta) , \qquad (1)$$

where θ is the angle subtended at the M dwarf by the Earth and the white dwarf. Performing the required integration, we find

$$\Phi(\theta) = (1 + \cos\theta)/8 = (1 - \cos\phi \sin i)/8 , \qquad (2)$$

where ϕ is the orbital phase according to the same convention as that mentioned previously and i is the inclination.

Model B.—In this model, we assume that the Hα surface brightness of the illuminated hemisphere is constant, independent of both position and angle of viewing. This may be appropriate, if the optical depth in the Hα is very large and if the ionized layer is nearly isothermal. In this case, we again find that

$$\Phi(\theta) \propto 1 + \cos\theta .$$

Model C.—Here we retain assumption A2 but assume that the layer is optically *thick* in Hα. In this case, the formalism developed by Margon *et al.* (1977) may be applied to yield

$$\Phi(\theta) \propto \sin\theta + (\pi - \theta)\cos\theta .$$

VI. APPLICATION OF THE REPROCESSING MODELS

We first verify that the reprocessing hypothesis is energetically feasible, using model A above for convenience.

From the Hα equivalent widths and continuum intensities given by LM, we derive $S_{\rm H\alpha} \approx 5 \times 10^{-2}$ cm^{-2} s^{-1}. The EUV observations of Margon *et al.* (1976) allow us to estimate $S_{\rm EUV} \approx 5 \times 10^2$ cm^{-2} s^{-1}, after a somewhat uncertain correction for interstellar absorption. We take $A \approx 2a \sin i \approx 11\ R_\odot$ from our observations, and $R_M \approx 0.6\ R_\odot$ from LM's spectral classification and from Bopp's (1974) study of YY Gem. For the orbital phase of LM's observation, we estimate $\Phi(\theta) \approx 0.2$. From equation (1), then, we find $f = 0.17$. This is a plausible value in spite of the uncertainties involved in the determination.

For each model, our knowledge of $\Phi(\theta)$ allows us to estimate the orbital inclination from the data. In

models A and B we find, from a weighted least-squares fit, that $i = 60°$ $(+15°, -7°)$. The uncertainties here were derived similarly to those in the orbital parameters above and should represent approximate 90% confidence intervals. For model C, however, we find $i = 41°$ $(+11°, -7°)$. The best fit for each of these models is shown with the data in Figure 2. We note that model C gives the better fit; the weighted sum of the squares of the residuals for the best-fit model C is 28% smaller than that for model A.

VII. THE MASS OF THE WHITE DWARF

We may now estimate the mass of the white dwarf from the standard expression

$$\frac{(a_M \sin i^3)}{P^2} = \frac{M_W{}^3 \sin^3 i}{M_W + M_M},$$

where subscripts M and W refer to the M dwarf and the white dwarf, respectively, and the units are AU solar masses, and years. Clearly, our limit will depend on M_M; in what follows, we take this to be 0.60 $(+0.10, -0.30)$, again from LM's spectral type, Bopp (1974), and Allen (1973).

We can set a firm lower limit to M_W by letting both K and M_M go to their lower limits, and taking i to be 90°. This gives $M_W \geq 0.46$. For models A and B, we find $M_W = 0.67$ $(+0.14, -0.19)$;[2] we derive our upper and lower limits by letting K, M_W, and $\sin i$ all go to their appropriate limits. In a similar fashion, we find for model C that $M_W = 0.93$ $(+0.32, -0.31)$. The full range of masses possible under our models is thus $0.46 \leq M_W \leq 1.24$.

VIII. DISCUSSION

Because many parameters of the Feige 24 system are now well determined, we may ask what relevance this has to the theory of the late stages of stellar evolution. Although a detailed study is beyond the scope of this work, we point out a possible theoretical implication.

As Ritter (1976) has noted, white dwarfs of mass greater than $0.45\ M_\odot$, such as Feige 24, are not expected from the evolution of binary stars, *unless* the first mass exchange is delayed until after the onset of core helium burning. If mass exchange occurs before this, nearly the entire envelope of the red giant primary is stripped off, leaving a core of mass less than $0.45\ M_\odot$ (Kippenhahn, Kohl, and Weigert 1967). In order to delay mass transfer until after core helium burning begins, the initial binary separation must have been greater than $\sim 100\ R_\odot$. Thus we have evidence for substantial angular momentum loss. In Ritter's scenario for the formation of cataclysmic variable stars, this angular momentum loss continues, and a very close binary ($P \sim$ hours) results. Evidently, Feige 24 stopped short of this, as did BD +16°516 (Nelson and Young 1970; Hills and Dale 1974). Although Ritter's scenario may be correct in some cases, it is evidently not inevitably followed.

During the primary's giant phase, the M dwarf secondary may have accreted a considerable amount of material. It is not entirely clear whether the Kelvin-Helmholtz time for the resulting envelope is short compared with the estimated cooling time for the white dwarf, which should be $\sim 10^7$–10^8 yr (Lamb and Van Horn 1975). If the M dwarf has not had sufficient time to relax, we may see it slightly above the main sequence, whereas it would be less massive than we have inferred. Fortunately, our limits on M_W are only weakly dependent upon M_M, and our adopted lower value for M_M is considerably smaller than the likely value.

Our interpretation of the Feige 24 system implies that the M dwarf intercepts an EUV power equal to about half the bolometric luminosity of the M dwarf itself. Thus we expect the red continuum to vary with orbital phase at some level. This continuum variation may in fact be responsible for the scatter in photometric measurements of Feige 24 noted by Holm (1976). To search for this variation, we examined both red and blue patrol plates from the Harvard collection; unfortunately for our purposes, the latter are more numerous and sensitive than the former. Forty-two blue plates were examined from the period 1928–1977, with no variations found to a level of 0.1 mag; the uncertainties estimate is derived from the scatter in the individual magnitudes. Twenty-four red plates were measured from the period 1938–1977; again, there is no evidence of variability, to a limit of approximately 0.25 mag. A systematic program of red and infrared photoelectric photometry might well reveal periodic fluctuations at a lower amplitude.

We thank Dr. L. V. Kuhi for loaning us the spectra from the 1975–1976 season, and Drs. D. M. Popper and M. Hartoog for exchanging some observing time with us and for obtaining some of the plate material.

The experienced assistance of E. A. Harlan was important to this study. Tim Erickson wrote the radial velocity reduction program. We thank Drs. H. Spinrad, L. V. Kuhi, and R. Taam for useful discussions. J. R. T. is an NSF Graduate Fellow. This work has been supported primarily by NSF grant AST 75-03735A01. One of us (B. M.) thanks Drs. M. and Wm. Liller for their hospitality at the Harvard plate collection, and acknowledges the partial financial support of NASA grant NSG 4159.

[2] Since only one side of the M dwarf produces emission lines, our radial velocity curve underestimates the amplitude of the M dwarf's motion. We have added $0.30\ R_\odot \sin i$ to our observed $a \sin i$ to correct approximately for this effect. This makes a small ($\sim 0.004\ M_\odot$) difference in our final mass estimate.

REFERENCES

Allen, C. W. 1973, *Astrophysical Quantities* (3d ed.; London: Athlone Press).
Bopp, B. W. 1974, *Ap. J.*, **193**, 389.
Cash, W. 1978, in preparation.
Cruddace, R., Paresce, F., Bowyer, S., and Lampton, M. 1974, *Ap. J.*, **187**, 497.

Eggen, O., and Greenstein, J. L. 1965, *Ap. J.*, **141**, 83.
Feige, J. 1958, *Ap. J.*, **128**, 267.
Hills, J. G., and Dale, T. M. 1974, *Astr. Ap.*, **30**, 135.
Holm, A. V. 1976, *Ap. J. (Letters)*, **210**, L87.
Kippenhahn, R., Kohl, K., and Weigert, A. 1967, *Zs. Ap.*, **66**, 58.
Lamb, D. Q., and Van Horn, H. M. 1975, *Ap. J.*, **200**, 306.
Liebert, J., and Margon, B. 1977, *Ap. J.*, **216**, 18 (LM).
Margon, B., Lampton, M., Bowyer, S., Stern, R., and Paresce, F. 1976, *Ap. J. (Letters)*, **210**, L79.
Margon, B., Nelson, J., Chanan, G., Thorstensen, J. R., and Bowyer, S. 1977, *Ap. J.*, **216**, 811.
Nelson, B., and Young, A. 1970, *Pub. A.S.P.*, **82**, 699.
Oke, J. B. 1974, *Ap. J. Suppl.*, **27**, 21.
Ritter, H. 1976, *M.N.R.A.S.*, **175**, 279.

STUART BOWYER, PHILIP A. CHARLES, and JOHN R. THORSTENSEN: Space Sciences Laboratory, University of California, Berkeley, CA 94720

BRUCE MARGON: Department of Astronomy, University of California, Los Angeles, CA 90024